Dynamics of the plane and solitary waves in a Noguchi network: Effects of the nonlinear quadratic dispersion

S A T Fonkoua[1], M S Ngounou[1], G R Deffo[2], F B Pelap[2,†], S B Yamgoue[3], and A Fomethe[2]

[1] Unité de Recherche de Matière Condensée d'Electronique et de Traitement du Signal (UR-MACETS), Faculté des Sciences,
Université de Dschang, BP 67 Dschang, Cameroun

[2] Unité de Recherche de Mécanique et de Modélisation des Systèmes Physiques (UR-2MSP), Faculté des Sciences,
Université de Dschang, BP 69 Dschang, Cameroun

[3] Department of Physics, Higher Teacher Training College Bambili, University of Bamenda, P.O. Box 39 Bamenda, Cameroon

We consider a modified Noguchi network and study the impact of the nonlinear quadratic dispersion on the dynamics of modulated waves. In the semi-discrete limit, we show that the dynamics of these waves are governed by a nonlinear cubic Schrödinger equation. From the graphical analysis of the coefficients of this equation, it appears that the nonlinear quadratic dispersion counterbalances the effects of the linear dispersion in the frequency domain. Moreover, we establish that this nonlinear quadratic dispersion provokes the disappearance of some regions of modulational instability in the dispersion curve compared to the results earlier obtained by Pelap *et al.* (*Phys. Rev. E* **91** 022925 (2015)). We also find that the nonlinear quadratic dispersion limit considerably affects the nature, stability, and characteristics of the waves which propagate through the system. Furthermore, the results of the numerical simulations performed on the exact equations describing the network are found to be in good agreement with the analytical predictions.

1. Introduction

During the last decades, the transmission electrical lines are increasingly used to study the behavior of the nonlinear dispersive media. Indeed, since the pioneering work of Hirota and Zuzuki[1] on electrical lines simulating the propagation of solitons in the atomic lattice of Toba,[2] the nonlinear transmission lines (NLTLs) have created passion and debate. Therefore, several models have been proposed in order to explain various physical phenomena in different branches of science. Indeed, Nejoh proposed a new type of nonlinear transmission line to describe the density depression and the collisionless shock wave in plasmas.[3] Twenty years later, Enjieu *et al.* modeled the nonlinear dynamics of plasma by using an anharmonic oscillator.[4] In the same spirit, Ainamon *et al.* studied the nonlinear dynamics of polarization oscillations of certain materials when they are subjected to the action of an electromagnetic wave modeled by the multi-frequency forced Duffing equation.[5] More recently, Makenne *et al.* exploited electrical lines to simulate periodic and chaotic motions of plants under the action of the wind.[6] Ndzana *et al.* also studied the dynamics of ionic waves in a microtubule modeled by a nonlinear resistor, inductor, and capacitor transmission line.[7] These few investigations partially justify the interest given to the electrical transmission lines since the first line of Hirota and Suzuki.

On the other hand, Noguchi built a new type of electrical transmission line to study experimentally the propagation of the first-order KdV solitons.[8] This network was also exploited to examine experimentally the properties of the second-order KdV solitons by using a new potential that generalized the Toda potential.[9] Based on the modified Noguchi line with linear dispersion, Pelap and Faye established a generalized criterion for the Benjamin–Feir instability and determined the exact solutions of the wave equation that governed the dynamics of the network.[10] Ndzana *et al.* considered a discrete dissipative Noguchi network for investigating the modulational instability (MI) phenomenon as well as the chaotic behavior of this dispersive medium.[11] Recently, the dynamics of elliptical waves in the same line was checked by other authors.[12] While examining the Noguchi network with nonlinear dispersion, Yamgoue *et al.* proposed exact solitary wave solutions of a nonlinear Schrodinger equation model with saturable-like nonlinearities.[13] More recently, Deffo *et al.* introduced a new model of two-dimensional Noguchi nonlinear electrical network and showed that the dynamics of small amplitude signals are described by a $(2+1)$-dimensional Zakharov–Kuznetsov equation type.[14] Several other variants of Noguchi nonlinear electrical transmission lines have also been proposed in the literature.[15,16]

The models studied above have led to very interesting and encouraging results. However, these models largely consider a linear dispersion in NLTLs, which limits the applicability of the established results to only a few physical phenomena.

http://iopscience.iop.org/cpb   http://cpb.iphy.ac.cn

For example, the NLTLs with linear dispersion give a good description of the dynamics of the classical soliton while they fail to describe the compact soliton.[17] Likewise, several interesting phenomena in NLTLs cannot be produced by the linear dispersion alone.[18] In addition, the few studies reported on NLTLs with nonlinear dispersion overlook the effects of this nonlinearity.[13,17]

In this work, we consider a modified Noguchi electrical transmission line with a nonlinear quadratic dispersion and examine the new features of this factor on the dynamics of modulated waves traveling in the network. This paper is organized as follows. In Section 2, we give a brief description of the model under consideration and find the differential difference equations governing its dynamics. Then, we call the semi-discrete approximation to establish that the dynamics of the modulated waves is described by an equation of the NLS type. In Section 3, we discuss the impact of the nonlinear quadratic dispersion both on the frequency domain of the dispersion curve and on the appearance of the modulational instability phenomenon. Numerical simulations are carried out in Section 4 to verify the accuracy of the analytical predictions built within this paper. Concluding notes are given in Section 5.

2. Model description and equation of the motion

2.1. Model description and basic equations

The physical model considered within this paper consists of many identical LC blocks connected as illustrated in Fig. 1. Each block contains a linear inductor L_s and a nonlinear capacitor $C_s(V)$ mounted in parallel in the series branch, and a nonlinear capacitor $C_p(V)$ in the shunt branch. We assume that the capacitance–voltage relationships are[19,20]

$$
\begin{aligned}
C_p (V_n + V_0) &= C_{0p} \left(1 - 2\alpha V_n + 3\beta V_n^2 \right), \\
C_s(V_n) &= C_{0s}(1 - 2\eta V),
\end{aligned}
\tag{1}
$$

where C_{0s} and C_{0p} are the respective limiting values of these capacitances when the voltages across them are infinitesimally small. The grandeurs α and η are the nonlinear quadratic coefficients, while β defines the cubic coefficient of nonlinearity.
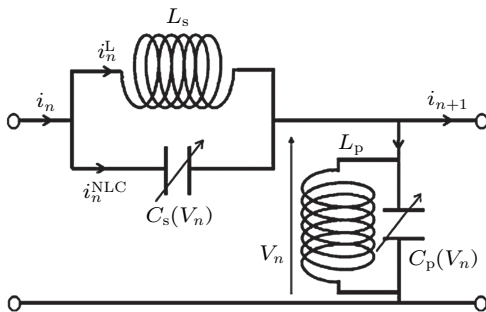

Fig. 1. Schematic representation of a unit cell. The dispersive nonlinear electrical transmission line is made of n identical units.

By applying the Kirchhoff's law to the circuit of Fig. 1, we obtain the following set of fundamental equations that describes the propagation of the voltage $V_n(t)$ in the network:

$$
\begin{aligned}
&\frac{d^2}{dt^2} \left(V_n - \alpha V_n^2 + \beta V_n^3 \right) + \omega_0^2 V_n \\
&= \left(u_0^2 + C_{0r} \frac{d^2}{dt^2} \right) (V_{n-1} + V_{n+1} - 2V_n) \\
&\quad + \eta C_{0r} \frac{d^2}{dt^2} \left[(V_n - V_{n+1})^2 - (V_{n-1} - V_n)^2 \right], \\
&n = 1, 2, \ldots, N,
\end{aligned}
\tag{2}
$$

where N and $C_{0r} = C_{0s}/C_{0p}$ represent, respectively, the number of cells considered and the dimensionless constant, while $\omega_0^2 = 1/L_p C_{0p}$ and $u_0^2 = 1/L_s C_{0p}$ designate the characteristic frequencies of the system.

In the linear domain of V_n, i.e., neglecting the terms of power greater than 1, and assuming a sinusoidal wave in which V_n is proportional to $\exp(i(kn - \omega t))$, we get a linear dispersion relation of the following form:

$$
\omega^2 = \frac{\omega_0^2 + 4u_0^2 \sin^2 (k/2)}{1 + 4C_{0r} \sin^2 (k/2)},
\tag{3}
$$

in which ω and k are, respectively, the angular frequency and wave number of the carrier wave. This dispersion relation is plotted in Fig. 2 for k chosen in the first Brillion zone $(0 \leqslant k \leqslant \pi)$. This representation clearly shows that our network is a pass-band filter with the lower cut-off frequency $f_0 = \omega_0/2\pi$ and the upper cut-off frequency $f_c = \sqrt{(\omega_0^2 + 4u_0^2)/(1 + 4C_{0r})}/2\pi$ which deals with the discrete nature of the line. Let us stress that f_c is inversely proportional to the reduced capacitance C_{0r}. Thus, the cut-off frequency f_c decreases with the growth of C_{0r}. This result means that the band-pass frequency of the nonlinear dispersion Noguchi filter decreases with the increase of C_{0r} and becomes more selective in terms of frequency. We could also note that the upper gap zone increases for nonzero values of C_{0r}. Therefore, the model is also appropriate for the investigation of the upper gap soliton dynamics.[19]
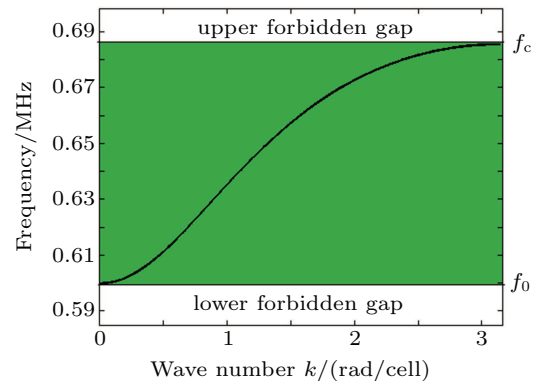

Fig. 2. The linear dispersion curve of the network with wave vector k (rad/cell) for $C_{0r} = 0.3$, $u_0 = 2.5786 \times 10^6$ rad/s, and $\omega_0 = 3.7689 \times 10^6$ rad/s.

The corresponding linear group velocity associated to the wave packet is defined below

$$\mu = \frac{d\omega}{dk} = \frac{1}{\omega} \frac{\left(u_0^2 - C_{0r}\omega^2\right)\sin(k)}{1 + 4C_{0r}\sin^2(k/2)}, \tag{4}$$

and drawn in Fig. 3 for the parameters of Fig. 2. It appears in the curve that the growth of C_{0r} induces a decrement of this velocity.[19]
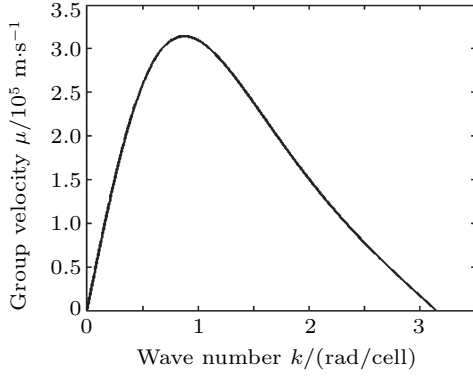

Fig. 3. Group velocity obtained for the parameters defined in Fig. 2.

2.2. Derivation of the cubic nonlinear Schrödinger equation

In this subsection, our attention is focused on the derivation of the cubic nonlinear Schrödinger equation describing the propagation of the modulated waves in the network. During this derivation, we assume that the envelope of the wave varies in time and space with regard to a given carrier wave with angular frequency ω and wave number k. To achieve this end, we call the reductive perturbation method in the semi-discrete limit to expand the voltage in the general form[19]

$$V_n(t) = \varepsilon V_{11}\,e^{i\theta} + \varepsilon^2(V_{20} + V_{22}\,e^{i\theta}) + \cdots + cc, \tag{5}$$

where θ defines the phase, ε is a small parameter, and "cc" stands for the complex conjugate of the preceding expression. Expression (5) includes the fast local oscillation through the dependence of the phase on $\theta = kn - \omega t$ and then preserves the discrete character of the system, while the dependence of the envelope part described by the function $V_{ij}(x,\tau)$ of the slow variables $\tau = \varepsilon^2 t$ and $x = \varepsilon(n - \mu t)$ takes care of the slow variation in amplitude. Substituting Eq. (5) into Eq. (2), we derive different equations as power series of ε. Therefore, the coefficients proportional to $\varepsilon^2 \exp(2i\theta)$ and $\varepsilon^4 \exp(0i\theta)$ respectively give

$$V_{20} = C_{20}\,|V_{11}|^2, \quad V_{22} = C_{22}V_{11}^2, \tag{6}$$

with

$$C_{22} = \frac{4\omega^2\left[16iC_{0r}\eta\sin^3\left(\frac{k}{2}\right)\cos\left(\frac{k}{2}\right) - \alpha\right]}{\left(4u_0^2 - 16C_{0r}\omega^2\right)\sin^2(k) + \omega_0^2 - 4\omega^2}, \quad C_{20} = \frac{2\alpha\mu^2}{\mu^2 - u_0^2}.$$

Using the above relations together with the coefficients proportional to $\varepsilon^3 \exp(i\theta)$ leads to the following equation governing the slow envelope evolution:

$$i\frac{\partial A}{\partial \tau} + P\frac{\partial^2 A}{\partial x^2} + Q|A|^2 A = 0, \tag{7}$$

where

$$P = \frac{M_1 - M_2 - \mu^2 M_0}{2\omega M_0}, \quad Q = \frac{N_1}{N_0 M_0} + \frac{N_2}{N_0 M_0\left(\mu^2 - u_0^2\right)} + \frac{3\beta\omega}{2M_0},$$

with $M_0 = 4C_{0r}\sin^2(k/2) + 1$, $M_1 = \left(u_0^2 - C_{0r}\omega^2\right)\cos(k)$, $M_2 = 4C_{0r}\omega\mu\sin(k)$,

$$N_0 = (4u_0^2 - 16C_{0r}\omega^2)\sin^2(k) + \omega_0^2 - 4\omega^2,$$
$$N_1 = 256\omega^3 C_{0r}^2\eta^2\sin^4(k/2)\sin^2(k),$$
$$N_2 = 4\omega^3\alpha^2\left(\mu^2 - u_0^2\right) - 2\omega\mu^2\alpha^2 N_0.$$

Equation (7) is a nonlinear cubic Schrödinger equation in which the parameters P and Q define the linear group velocity dispersion and the self-phase modulation (SPM), respectively. Physically, the first measures the wave dispersion while the second determines how the wave frequency is amplitude modulated. Setting $\eta = 0$, the first term of the SPM equals zero and one recovers the NLS equation established in Ref. [15].

3. Modulational instability phenomenon

3.1. Generalities

Modulational instability (MI) is a phenomenon that results from the interplay between nonlinearity and either the dispersion in the time domain or the diffraction in the spatial domain. It has been studied in various fields of science, namely, nonlinear optics,[21] condensed matter physics,[22] plasma physics,[23] and biophysics,[24] just to name a few. These investigations indicate that the MI phenomenon is an underlying physical mechanism which has several advantages. For instance, it is indispensable for understanding the relevant dynamic processes in the Bose–Einstein condensates systems which include domain formation, generation and propagation of soliton waves.[25] Similarly, MI is an indicator of the presence of discrete solitons in discrete dissipative systems and can be exploited to generate a soliton train at high repetition rate.[26] In inhomogeneous nonlinear systems, MI may be considered as the leading mechanism for energy localization as well as the formation of traveling intrinsic localized modes.[27]

In the NLS models, this phenomenon occurs if the product PQ is positive. In fact, the nonlinear dispersion relation is given by

$$\Omega^2 = K^2 P^2(K^2 - K_{cr}^2), \tag{8}$$

with $K_{cr}^2 = 2QA_0^2/P$. The grandeurs K and Ω designate, respectively, the wave number and the angular frequency of the perturbation. The plane wave is unstable against small modulation if the perturbation diverges with time, that is $K^2 - K_{cr}^2 <$

0. In this case, the angular frequency of the perturbation is complex and its imaginary part is considered as a measure of the growth rate of the perturbation defined as

$$g_0 = \left[K^2 P^2 (K_{cr}^2 - K^2)\right]^{1/2}. \tag{9}$$

Equation (8) shows that, for a wave propagating in the system to become unstable, it is necessary that $K_{cr}^2 > K^2$. K_{cr}^2 is an explicit function of P and Q, and depends implicitly on the network parameters. Hereafter, according to the wave number K, we will investigate numerically the role played by the nonlinear dispersion parameter η on the modulational instability phenomenon. Let us remind that any plane wave propagated in the line will be unstable if $PQ > 0$ and its wave number included in the fundamental gain band $K \in]0, K_{cr}]$.

3.2. Effects of the nonlinear quadratic dispersion

To clearly establish the effect of the nonlinear quadratic dispersion parameter η on the dynamics of waves in the network, we check the evolution of the coefficients of Eq. (7) and their product for the wave number of the signal chosen in the first Brillouin zone. This exam is done for null and non zero values of the nonlinear quadratic dispersion parameter. In fact, it is well-known that if $PQ < 0$, the plane wave remains stable during its motion in the system and equation (7) admits a dark soliton solution. On the other hand, when $PQ > 0$, the network can exhibit an instability that leads to a self-induced modulation of an input plane wave and the solution of Eq. (7) is a bright soliton. Since the dispersion coefficient P does not depend on η, we only draw the nonlinear coefficient Q and the product PQ with the parameters[16] $\alpha = 0.21$ V^{-1}, $\beta = 0.0197$ V^{-2}, $L_s = 470$ μH, $L_p = 220$ μH, $C_{0s} = 96$ pF, $C_{0p} = 320$ pF and for various values of parameter η picked in the literature,[28,29] namely, 0.16 V^{-1}, 0.21 V^{-1}, and 0.25 V^{-1}.

Figure 4 displays the behavior of Q versus the wave number k for four values of η. These curves indicate that, by neglecting the effects of the nonlinear quadratic dispersion and the linear capacitor (Fig. 4(a)), Q remains negative independently of the value of k. If the effect of the linear capacitor is checked alone (Fig. 4(b)), Q vanishes for wavelengths $k = 1.125$ and $k = 2$. It is negative in the domains $0 < k < 1.125$ and $2 < k < \pi$ and positive in the region $1.125 < k < 2$. For nonzero nonlinear quadratic component of the capacitor, the SPM is negative for all values of the wave number (Fig. 4(c)). This result is similar to that of Fig. 4(a) with low values of Q otherwise the parameter η does not greatly impact the SPM.

Figure 5 displays the plots of the product PQ (left plots) as a function of the signal frequency and the corresponding dispersion relation (right plots) that include the different regions of modulational stability/instability phenomenon. Indeed, three cases appear from our finding: the upper panel

that links with $C_{0s} = 0$ and $\eta = 0$, the middle panel that corresponds to $C_{0s} \neq 0$ and $\eta = 0$, and the bottom panel that deals with $C_{0s} \neq 0$ and $\eta \neq 0$.
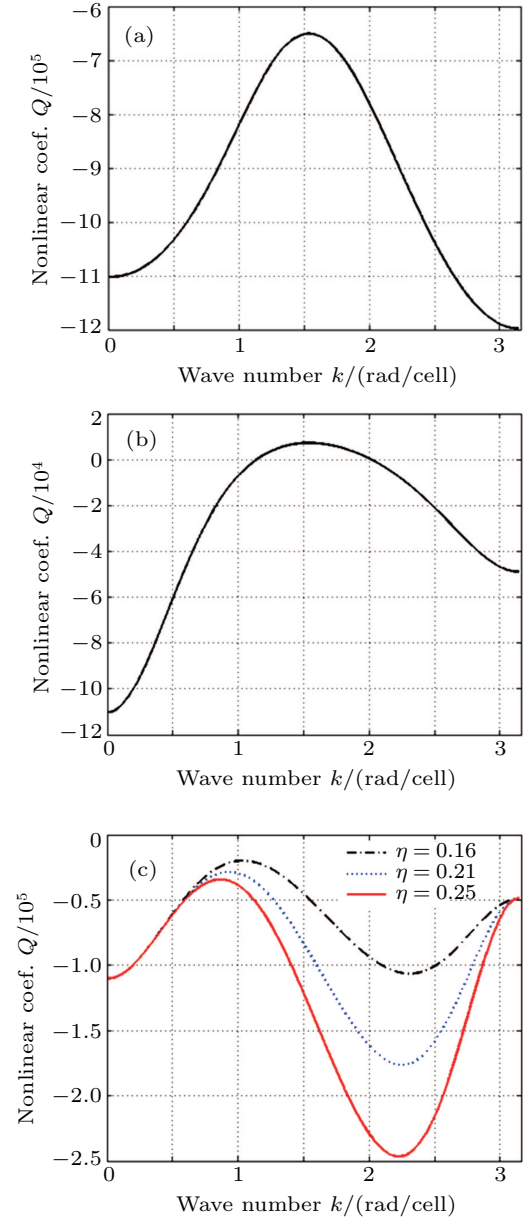

Fig. 4. Nonlinear coefficient Q in terms of the wave number for the parameters of Fig. 2 with $\alpha = 0.21$ V^{-1} and $\beta = 0.0197$ V^{-2}: (a) without capacitor C_s in series branches, (b) and (c) with $C_s \neq 0$ for $\eta = 0$ and $\eta \neq 0$, respectively.

First, we start with the case $C_{0s} = 0$ and $\eta = 0$ dealing with the absence of the capacitor in the series branch of Fig. 1.

Here, there exist two domains in which the product PQ can be positive or negative (Figs. 5(a) and 5(b)):

(i) $f \in [f_0, f_{01}]$, $PQ < 0$, the wave plane remains stable under modulation and the solutions of the NLS equation are dark solitons;

(ii) $f \in [f_{01}, f_{c1}]$, $PQ > 0$, the wave plane is unstable under modulation and the solutions of the NLS equation are envelope solitons.
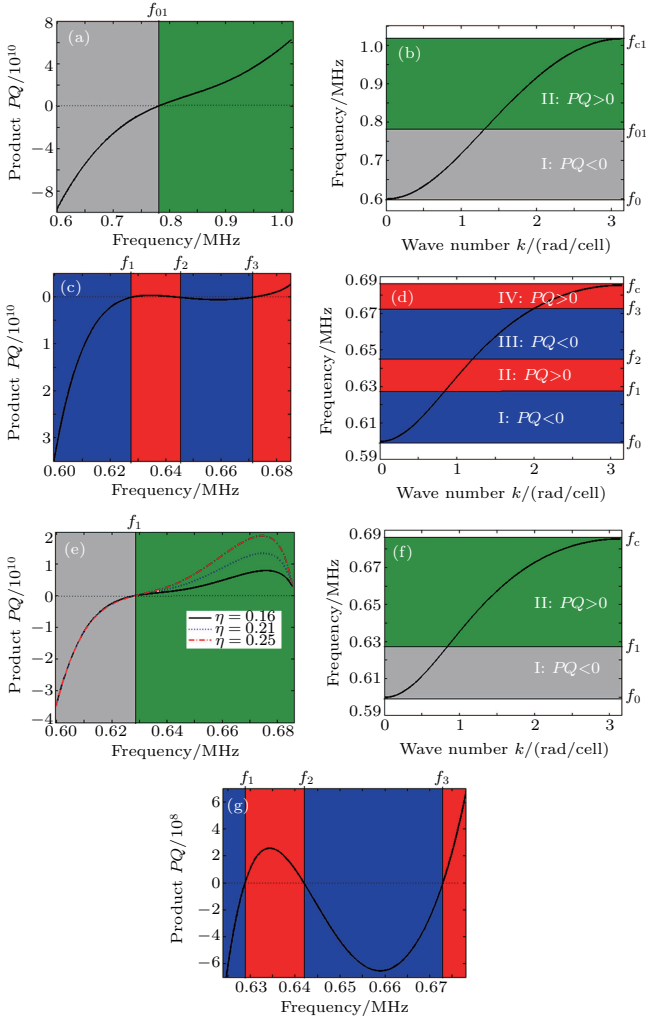
Fig. 5. Product PQ (left plots) and linear dispersive curves (right plots) in terms of the frequency $f = \omega/2\pi$ and the wave number k, respectively. These graphs are obtained with the given parameters of Fig. 4 for different input parameters: (a) and (b) without the effect C_s in the series branch, (c) and (d) the nonlinear quadratic component of the capacitor C_s is neglected ($\eta = 0$), (e) and (f) with the effects of the nonlinear quadratic component of C_s ($\eta \neq 0$). Panel (g) is the zoomed view of the curve in (c).

Next, we consider the case where the capacitor in the series branch of Fig. 1 is linear, that is $\eta = 0$. Then, there exist four domains in which the product PQ is either positive or negative (Figs. 5(c) and 5(d):

(i) $f \in [f_0, f_1]$, $PQ < 0$, the wave plane is modulationally stable and the solutions of Eq. (7) are hole solitons;

(ii) $f \in [f_1, f_2]$, $PQ > 0$, the wave plane is modulationally unstable and equation (7) admits the bright solitons solutions;

(iii) $f \in [f_2, f_3]$, $PQ < 0$, the wave plane remains stable under modulation and the solutions of Eq. (7) are dark solitons;

(iv) $f \in [f_3, f_c]$, $PQ > 0$, the wave plane is unstable under modulation and the solutions of Eq. (7) are envelope solitons.

Finally, when the capacitor in the series branch of Fig. 1 is nonlinear, that is, the nonlinear quadratic dispersion is considered ($\eta \neq 0$), there exist only two frequency domains where the product PQ is positive or negative (Figs. 5(e) and 5(b)), that is,

(i) $f \in [f_0, f_1]$, $PQ < 0$, the wave plane remains modulationally stable and equation (7) possesses the hole solitons solutions;

(ii) $f \in [f_1, f_c]$, $PQ > 0$, the wave plane is unstable under modulation and the NLS equation admits envelope solitons solutions.

From the above-mentioned cases, it is clear that the nature of the capacitor in the series branch of Fig. 1 strongly affects the properties and the dynamics of the waves in a modified Noguchi electrical transmission line. In particular, we recover that the network has two frequency regions in the absence of the capacitor C_s in the series branch. When we consider the effect of the linear component of the capacitor C_s and neglect that of the nonlinear quadratic component, there appear four frequency domains in which the network can exhibit modulational stability or instability. Therefore, the linear component of the capacitor contributes to increase the number of the stability and instability domains in the network.[15,19] Moreover, when the nonlinear component of the capacitor (i.e., the quadratic nonlinearity) is included, the number of the frequency domains in the network decreases to two and equals the results obtained for the case where the capacitor C_s in the series branch is neglected. This last result induces the possibility that the nonlinear quadratic component can be used to balance the effect of the linear component of the capacitor C_s with suitable values of considered network parameters. Another striking and important result of this analysis is the possibility to obtain two different solitary (one bright and one dark) signals at the same frequency by a judicious choice of the nonlinear quadratic dispersion parameter.

4. Numerical investigation

We intend to perform numerical simulations on the exact discrete Eq. (2) governing the wave propagation in the network in order to test the veracity of the analytical computations previously made. To this end, the fourth order Runge–Kutta algorithm is called for the direct integration of Eq. (2). Our analysis is carried out on a discrete nonlinear electrical transmission line (Fig. 1) made of 1200 cells and fixed boundary conditions. The parameters of the nonlinear capacitor in the shunt branch are $\beta = 0.0197$ V^{-2}, $\alpha = 0.21$ V^{-1}, $C_{0p} = 320$ pF, and $L_p = 0.22$ mH. For the characteristic parameters of the capacitor in the series branch, we use $C_{0s} = 96$ pF, $L_s = 0.47$ mH, $\eta = 0.21$ V^{-1} and two values of the quadratic parameter, that is, $\eta = 0$ V^{-1} and $\eta = 0.21$ V^{-1}. With these numerical values, the following characteristics of the network are obtained: $\omega_0 = 3.7689 \times 10^6$ rad/s and $u_0 = 2.5786 \times 10^6$ rad/s, $C_{0r} = 0.3f_0 = \omega_0/2\pi = 599.84$ kHz, and $f_c = \omega(k=\pi)/2\pi = 685.39$ kHz. We will examine numerically the modulational instability phenomenon and the propagation of the envelope soliton in the network.

4.1. Behavior of plane waves in the network

We start by reminding that a plane wave introduced in the line becomes unstable in the focusing media ($PQ > 0$) and remains stable in the defocusing media ($PQ < 0$). To numerically check it, the following signal is applied at the input of the line:

$$V(t) = V_m [1 + m \cos(2\pi f_m t)] \cos(2\pi f_p t), \qquad (10)$$

where $f_m = 8$ kHz is the modulation frequency, $V_m = 0.5$ V is the amplitude of the wave, $m = 0.01$ is the modulation rate, and f_p is the carrier frequency whose value is taken in a given frequency domain. For the effectiveness of these simulations, the cells 1, 250, and 450 are arbitrary chosen to observe the behavior of the wave during its progression in the system. Two different cases are considered.
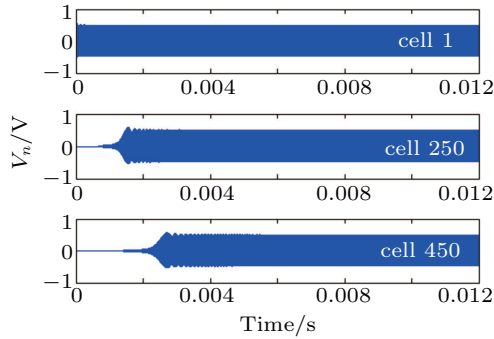

Fig. 6. Modulational stability behavior of the plane wave with the frequency $f_p = 667.30$ kHz in the network that belongs to domain III of the dispersion curve (Fig. 5(d)).
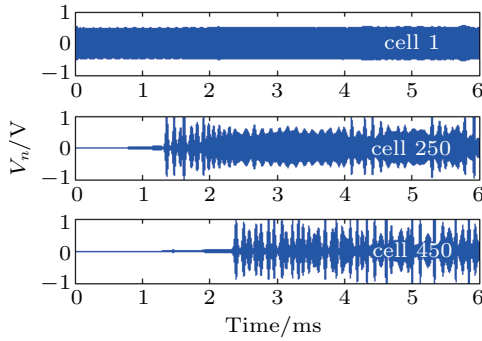

Fig. 7. Modulational instability behavior of the plane wave in the line with the frequency $f_p = 667.30$ kHz belonging to the domain II of the dispersion curve (Fig. 5(f)). We observe a modulation during the motion of the wave.

As a first example of the outcome of these experiments, figure 6 displays the evolution of a plane wave with the frequency $f_p = 667.30$ kHz chosen in the domain III of Fig. 5(d) where the analytical analysis predicted a modulational stability. These curves show that the solution (10) remains stable under modulation, agreeing perfectly with the analytical predictions.

For further illustrations, the same carrier frequency $f_p = 667.30$ kHz of the plane is chosen but in domain II of Fig. 5(f) where the analytical investigation predicted a modulational instability phenomenon induced by the presence of the nonlinear quadratic dispersion. The motion of the plane wave in the

line under such conditions is depicted in Fig. 7 that allows observing the modulation instability behavior of the plane wave. These results which agree with the analytic prediction confirm the impact of the nonlinear quadratic dispersion on the properties of the network considered in this paper.

4.2. Propagation of envelope solitons

To experience the transmission of the envelope soliton through our model for several bands of frequencies dictated by Fig. 5, we excite one extremity of the line with an envelope solution of the NLS equation[30]

$$V_n(t) = V_0 \operatorname{sech}[\gamma(n - \mu_s t)] \cos(K_s n - \omega_s t), \qquad (11)$$

where $\gamma = (V_0/2)\sqrt{Q/2P}$, $\mu_s = \mu + v_e P\varepsilon^2$, $K_s = k + v_e/2$, and $\omega_s = \omega + v_e(\mu + v_c P\varepsilon^2)/2$. Here, v_e and v_c are the amplitude and phase velocities of the soliton, respectively.

In order to avoid signal reflection that disturbs the accurate observation of the wave propagation in the network, the voltage across the other extremity is set to zero and the experiment is run for a sufficiently long time. Results of the numerical simulations are given in Figs. 8 and 9.

In the first case (Fig. 8), the signal with the frequency $f = 635.13$ kHz is taken in the focusing domains II of Figs. 5(d) and 5(f). It appears that data can be carried out through the network of Fig. 1 without distortion. Nevertheless, one observes that the nonlinear quadratic dispersion influences the width of the solitary wave during its propagation. Hence, this parameter can be used to control the shape of this wave.
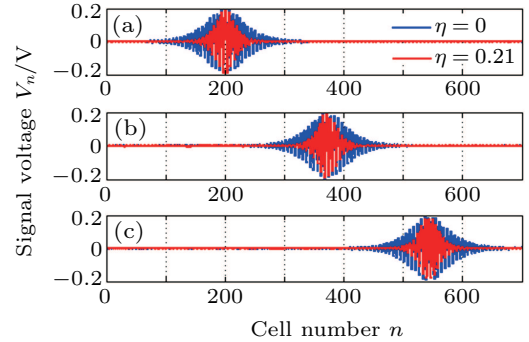

Fig. 8. Propagation of the bright soliton solution of Eq. (2) in the network with $f = 635.13$ kHz taken in the focusing domains II of Figs. 5(d) and 5(f) which correspond respectively to the case with (red curves) and without (blue curves) nonlinear quadratic dispersion: (a) the initial signal voltage is located at cell $n_0 = 200$ with amplitude $V_0 = 0.2$ V, (b) and (c) explain the signal at given time of propagation: $t_1 = 0.556$ ms and $t_2 = 1.1$ ms, respectively.

On the other hand, figure 9 presents the behavior of the bright soliton with the frequency $f = 648.66$ kHz (taken in the focusing domain II of Fig. 5(f)) in the nonlinear transmission line. These curves show that the initial electrical signal voltage propagates with constant amplitude and without distortion of its shape. This result corroborates with the analytical prediction. At this frequency, the modified Noguchi network without the nonlinear quadratic dispersion cannot support the envelope

solitons (Fig. 5(d)), but this result exposes once again, the impact of this nonlinear dispersion on the dynamic of this system.
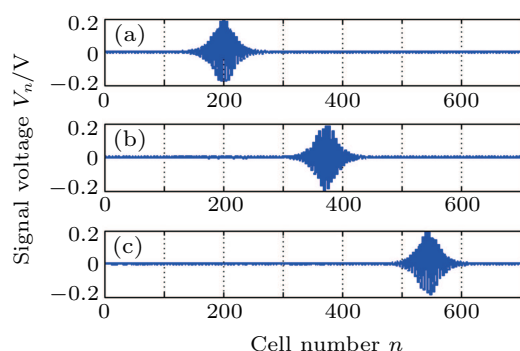

Fig. 9. Propagation of the bright solitary wave through the network with $f = 648.66$ kHz taken in the focusing domain II of Fig. 5(f) with nonlinear quadratic dispersion: (a) the initial signal voltage is located at cell $n_0 = 200$ with amplitude $V_0 = 0.2$ V, (b) and (c) show the signal at given time of propagation: $t_1 = 0.6$ ms and $t_2 = 1.2$ ms, respectively.

5. Conclusion

We have studied analytically and numerically the effects of the nonlinear quadratic dispersion on the dynamics of modulated waves in a modified Noguchi transmission line. We have demonstrated through the reductive perturbation approach that the propagation of modulated waves in the network is described by the nonlinear cubic Schrödinger equation. The analytic expressions of its various coefficients were established and their analyses revealed that the nonlinear quadratic dispersion has profoundly modified the dynamics of the system, results which contrast with the case of linear dispersion previously obtained. For instance, our investigations have shown that this nonlinear quadratic component counterbalances the effects of the linear component. Moreover, we have found that the quadratic nonlinear dispersion reduces the MI domains to two regions, unlike four in Ref. [12] and allows the possible propagation of bright and dark solitary signals at the same frequency through the network. Numerical simulations performed in the framework of the nonlinear lattice equation have led to outcomes that are in perfect agreement with the analytical predictions. In addition, our study can be useful to make a better choice of the quadratic parameter and to help a better understanding of the results of experiments of the propagating modulated wave in the transmission lines with nonlinear dispersion.

References

[1] Hirota R and Suzuki K 1970 *J. Phys. Soc. Jpn.* **28** 1366
[2] Toda M 1967 *J. Phys. Soc. Jpn.* **23** 501
[3] Nejoh Y 1987 *J. Phys. A: Math. Gen.* **20** 1733
[4] Afshari E and Hajimiri A 2005 *IEEE J. Solid State Circuits* **40** 744
[5] Enjieu Kadji H G, Nana Nbendjo B R, Chabi Orou J B and Talla P K 2008 *Phys. Plasmas* **15** 032308
[6] Makenne Y L, Kengne R and Pelap F B 2019 *Chaos Soliton. Fract.* **127** 70
[7] Ndzana I I F and Mohamadou A 2019 *Chaos* **29** 013116
[8] Noguchi A 1974 *Electron. Commun. Jpn. A* **57** 9
[9] Ichikawa Y H, Mitsuhaski T and Konno K 1976 *J. Phys. Soc. Jpn.* **41** 1382
[10] Pelap F B and Faye M M 2005 *J. Math. Phys.* **46** 033502
[11] Ndzana I I F, Mohamadou A and Kofane T C 2007 *J. Phys. D* **40** 3254
[12] Pelap F B, Kamga J H, Yamgoue S B, Ngounou S M and Fomethe A 2015 *Chin. J. Phys.* **53** 080701
[13] Yamgoue S B, Deffo G R, Talla-Tebue E and Pelap F B 2018 *Chin. Phys. B* **27** 126303
[14] Deffo G R, Yamgoue S B and Pelap F B 2018 *Phys. Rev. E* **98** 062201
[15] Kengne E, Lakhssassi A and Liu W M 2017 *Phys. Rev. E* **96** 022221
[16] Deffo G R, Yamgoue S B and Pelap F B 2018 *Eur. Phys. J. B* **91** 242
[17] Deffo G R, Yamgoue S B and Pelap F B 2019 *Phys. Rev. E* **100** 022214
[18] Nguetcho A S T, Nkeumaleu G M and Bilbault J M 2017 *Phys. Rev. E* **96** 022207
[19] Pelap F B, Kamga J H, Yamgoue S B, Ngounou S M and Ndecfo J E 2015 *Phys. Rev. E* **91** 022925
[20] Yamgoue S B, Deffo G R, Tala-Tebue E and Pelap F B 2018 *Chin. Phys. B* **27** 096301
[21] Abdullaev F K, Darmanyan S A and Garnier J 2002 *Prog. Opt.* **44** 303
[22] Malendevich R, Jankovic L, Stegeman G I and Aitchison J S 2001 *Opt. Lett.* **26** 1879
[23] Zakharov V and Ostrovsky L 2009 *Physica D* **238** 540
[24] Tabi C B, Mohamadou A and Kofane T C 2008 *J. Phys.: Condens. Matter* **20** 415104
[25] Mohamadou A, Wamba E, Doka S Y, Ekogo T B and Kofane T C 2011 *Phys. Rev. A* **84** 023602
[26] Mohamadou A, Kenfack-Jiotsa A and Kofane T C 2006 *Chaos Soliton. Fract.* **27** 914
[27] Abdoulkary S, Tabi C B, Doka S Y, Ndzana I I F, Kavitha L and Mohamadou A 2012 *J. Mod. Phys.* **3** 438
[28] Remoissenet M 1999 *Waves Called Solitons* (3rd Edn.) (Berlin: Springer-Verlag)
[29] Kengne E and Lakhssassi A 2015 *Phys. Rev. E* **91** 032907
[30] Togueu Motchey A B, Tchinang Tchameu J D, Fewo S I, Tchawoua C and Kofane T C 2017 *Commun. Nonlinear. Sci. Numer. Simulat* **53** 22